Helix Formation in Unsolvated Alanine-Based Peptides: Helical Monomers and Helical Dimers

Robert R. Hudgins and Martin F. Jarrold*

Contribution from the Department of Chemistry, Northwestern University, 2145 Sheridan Road, Evanston, Illinois 60208

Received November 19, 1998

Abstract: High-resolution ion mobility measurements and molecular dynamics simulations have been used to examine helix formation in protonated alanine-based peptides in a solvent-free environment. Protonated polyalanines, Ala_nH^+, with up to 20 residues do not form extended helices in a vacuum. However, experiment and theory indicate that the addition of a lysine to the C terminus ($Ac\text{-}Ala_n\text{-}LysH^+$) results in the formation of a stable monomeric helix for $n \geq 7$. This helix is stabilized by the protonated lysine side chain capping the C terminus and by the interaction of the charge with the helix dipole. If the lysine is moved to the N terminus ($Ac\text{-}LysH^+\text{-}Ala_n$) the helix-stabilizing factors are absent, and for $n < 13$ these peptides adopt globular conformations. For $n > 13$ only dimers are observed. The dimers appear to be helical, with the lysine from one peptide interacting with the C terminus of the other in a head-to-toe, "coiled-coil"-like arrangement of antiparallel helices. The transition from helical dimers to monomeric globules that occurs at $n = 13$ is partly driven by the entropy cost of dimerization. Dimers are also observed for the $Ac\text{-}Ala_n\text{-}LysH^+$ peptides. These dimers also appear to be helical and linked by the lysine of one peptide interacting with the C terminus of the other. However, here the helices adopt a nearly collinear (or vee-shaped) arrangement that minimizes unfavorable electrostatic interactions.

Introduction

Proteins can be thought of as aggregates of secondary structure.[1] Thus, understanding the factors responsible for the stability of different secondary structure elements within proteins and how they organize, is central to understanding protein structure. The α-helix is the most common short-range structural motif in proteins and the most important secondary structure element.[2] Helix propensities differ for different amino acids. Alanine has the highest helix propensity of the natural amino acids,[3−5] and helix formation in alanine-based peptides has been extensively studied in solution.[6−8] Here we describe a study of helix formation in alanine-based peptides in a solvent-free environment, in a vacuum. We anticipate that these in vacuo studies will provide insight into the role of the solvent in helix formation and ultimately provide an intrinsic thermodynamic scale for the helix propensities of the different amino acids.

We recently reported that protonated polyalanine peptides, Ala_nH^+, $n \leq 20$, adopt globular conformations in vacuo.[9] It appears that the charge destabilizes the helical conformation for these peptides. Here we describe studies of alanine polypeptides incorporating a single lysine. The addition of the lysine at the C terminus ($Ac\text{-}Ala_n\text{-}LysH^+$) results in a stable monomeric helix for $n \geq 7$. The protonated lysine side chain stabilizes the helical conformation by capping (hydrogen bonds to the backbone carbonyl groups at the end of the helix) and by the interaction of the charge with the helix dipole. A preliminary report of some of our results for monomeric $Ac\text{-}Ala_n\text{-}LysH^+$ peptides has been presented elsewhere.[10] In this paper we provide a full account, and describe measurements and molecular dynamics simulations for $Ac\text{-}LysH^+\text{-}Ala_n$ peptides, where the lysine is located at the N terminus. The helix-stabilizing features present for peptides with the lysine at the C terminus ($Ac\text{-}Ala_n\text{-}LysH^+$) are absent when the lysine is moved to the N terminus ($Ac\text{-}LysH^+\text{-}Ala_n$). For $n < 13$ the $Ac\text{-}LysH^+\text{-}Ala_n$ peptides adopt globular conformations, as predicted by molecular dynamics simulations. However, for $n > 13$ only dimers are observed. Molecular dynamics simulations and experimental measurements suggest that these are helical dimers with the protonated lysine from one peptide interacting with the C terminus of the other in a head-to-toe arrangement of antiparallel helices. Thus, $Ac\text{-}LysH^+\text{-}Ala_n$ peptides which do not form helical monomers are predominantly helical when aggregated into dimers. Dimers were also observed for the $Ac\text{-}Ala_n\text{-}LysH^+$ peptides. These dimers also appear to be helical and are linked by the protonated lysine from one peptide interacting with the C terminus of the other. Our results suggest that these dimers have a nearly collinear (or vee-shaped) arrangement of the helices.

A variety of experimental techniques have been used to deduce information about the gas-phase conformations of proteins, peptides, and their aggregates.[11−20] We have used high-resolution ion mobility measurements[21,22] in the studies de-

(1) Levitt, M.; Chothia, C. *Nature (London)* **1976**, *261*, 552.
(2) Chou, P. Y.; Fasman, G. D. *Biochemistry* **1974**, *13*, 222.
(3) Chakrabartty, A.; Baldwin, R. L. *Adv. Protein Chem.* **1995**, *46*, 141.
(4) O'Neil, K. T.; DeGrado, W. F. *Science* **1990**, *250*, 646.
(5) Lyu, P. C.; Liff, M. I.; Marky, L. A.; Kallenbach, N. R. *Science* **1990**, *250*, 669.
(6) Marqusee, S.; Baldwin, R. L. *Proc. Natl. Acad. Sci. U.S.A.* **1987**, *84*, 8898.
(7) Marqusee, S.; Robbins, V. H.; Baldwin, R. L. *Proc. Natl. Acad. Sci. U.S.A.* **1989**, *86*, 5286.
(8) Millhauser, G. L.; Stenland, C. J.; Hanson, P.; Bolin, K. A.; van de Ven, F. J. M. *J. Mol. Biol.* **1997**, *267*, 963.
(9) Hudgins, R. R.; Mao, Y.; Ratner, M. A.; Jarrold, M. F. *Biophys. J.*, **1999**, *76*, 1591.
(10) Hudgins, R. R.; Ratner, M. A.; Jarrold, M. F. *J. Am. Chem. Soc.* **1998**, *120*, 12974.

10.1021/ja983996a CCC: $18.00
Published on Web 03/25/1999

scribed herein. The mobility of an ion in the gas phase is a measure of how rapidly it moves through an inert buffer gas under the influence of a weak electric field. The mobility depends on the ion's collision cross section with the buffer gas: ions with compact conformations undergo fewer collisions and move more quickly than ions with more open conformations.[23−26] Structural information is deduced by comparing measured cross sections to orientationally averaged cross sections calculated for conformations derived from molecular dynamics (MD) simulations.

Ion Mobility Measurements

The high-resolution ion mobility apparatus used for these measurements has been described in detail previously.[21,22] Briefly, the apparatus consists of an electrospray source, coupled to a 63-cm drift tube, followed by a quadrupole mass spectrometer and an ion detector. The ions are electrosprayed in air and enter the apparatus through a 0.125-mm aperture. They initially enter a small differentially pumped volume where a substantial fraction of the air and solvent that comes in through the entrance aperture is pumped away, along with helium buffer gas which enters from the other side. The ions are drawn through this volume by an electric field and then enter a desolvation region which is maintained at room temperature. After passing through the desolvation region, the ions pass through the ion gate and enter the drift tube. The ion gate consists of a cylindrical channel, 0.5 cm in diameter and 2.5 cm long. A helium buffer gas flow of around 1800 sccm prevents solvent and air molecules from entering the drift tube from the desolvation region, while an electric field of 400 V cm^{-1} carries the ions through against the buffer gas flow. The drift tube has 46 drift guard rings, coupled to a voltage divider, to provide a uniform electric field along its length. A drift field of 160 V cm^{-1} was employed with a helium buffer gas pressure of around 500 Torr. After traveling along the length of the drift tube, some of the ions exit through a 0.125-mm diameter aperture and are focused into a quadrupole mass spectrometer. Following mass analysis, the ions are detected by an off-axis collision dynode and dual microchannel plates. Drift time distributions are recorded by switching the voltages on a pair of half plates in the ion gate so that a short packet of ions (usually 750 μs) is admitted to the drift tube. The arrival time distribution of the packet of ions is recorded at the detector with a multichannel scaler. The measured drift times, t_D, are converted into average collision cross sections using[27]

$$\Omega_{av}^{(1,1)} = \frac{(18\pi)^{1/2}}{16}\left[\frac{1}{m}+\frac{1}{m_b}\right]^{1/2}\frac{ze}{(k_B T)^{1/2}}\frac{t_D E}{L}\frac{1}{\rho} \quad (1)$$

In this expression, m and m_b are the masses of the ion and a buffer gas atom, ze is the charge on the ion, ρ is the buffer gas number density, L is the length of the drift tube, and E is the drift field.

Materials. Ac-Ala$_{13}$-Lys, Ac-Ala$_{19}$-Lys, Ac-Lys-Ala$_{13}$, and Ac-Lys-Ala$_{19}$ peptides with acetylated N termini were synthesized by Anaspec (Anaspec Inc., San Jose, CA) and used without purification. In each case there is a distribution of peptide sizes present because of inefficient coupling in the Fmoc synthesis. Furthermore, the peptides are slowly hydrolyzed in the strong organic acids used to dissolve them for electrospraying, and thus the distribution of peptide sizes present gradually shifts to smaller sizes. The presence of a distribution of sizes is not a concern in our measurements because specific peptides can be mass selected.

Molecular Dynamics Simulations. Information about the peptide conformations is obtained by performing molecular dynamics (MD) simulations and then calculating average cross sections for the structures sampled in the MD simulations for comparison with the measured cross sections. The MD simulations were performed using the PROSIS molecular modeling package with CHARMM-like potentials[28] using the 21.3 parameter set. The bond lengths were constrained by SHAKE[29] and the CH, CH_2, and CH_3 units were treated as united atoms. In both the Ac-Lys-Ala$_n$ and Ac-Ala$_n$-Lys peptides the protonation site is assumed to be the nitrogen in the lysine side chain (protonation at the N terminus is blocked by acetylation). The lysine side chain has the highest pK_a in solution, and gas-phase basicity measurements for individual amino acids and small peptides are consistent with protonation at the side chain amine.[30,31] The simulations were performed with a time step of 1 fs. A dielectric constant of 1, which is appropriate for small peptides in a vacuum, was used. Multiple simulations of 0.25−1.0 ns were performed at 300 K for each peptide. Some simulations were performed at temperatures up to 700 K to search the energy landscape and provide an indication of the stability of some of the conformations.

Cross sections were calculated using the trajectory method,[32] which is the most rigorous method currently available. Here the cross sections are calculated by propagating He atom classical trajectories within a He-polypeptide potential consisting of a sum of two-body Lennard−Jones interactions and ion-induced dipole interactions. The Lennard−Jones parameters used in the He-polypeptide potential were $\epsilon = 1.34$ meV and $r_o = 3.042$ Å for C, N, and O atoms with He, and $\epsilon = 0.65$ meV and $r_o = 2.38$ Å for H with He. The partial charges from the CHARMM 21.3 parameter set were employed for the ion-induced dipole interactions. Trajectory calculations are run for a wide range of impact parameters, relative velocities, and collision geometries in order to determine the cross section. Since the interatomic distances fluctuate somewhat during a molecular dynamics simulation, average cross sections were calculated by averaging over 50 conformations taken over a period of 60 ps after the system had equilibrated. In the work reported here, a total of 500 000 trajectories were run for each peptide or dimer and the average cross sections converged in all cases to within 1%. Normally we expect the calculated cross sections to be within a couple of percent of the measured ones, if the conformations used in the cross section calculations are correct. A cross section measurement is a relatively poor structural probe in the sense that a large number of geometries could be constructed with the same cross section. However, the number of geometries which are both low in energy and have the right cross section is much smaller; often there is only one such combination.

(11) Suckau, D.; Shi, Y.; Beu, S. C.; Senko, M. W.; Quinn, J. P.; Wampler, F. M.; McLafferty, F. W. *Proc. Natl. Acad. Sci. U.S.A.* **1993**, *90*, 790.
(12) Collings, B. A.; Douglas, D. J. *J. Am. Chem. Soc.* **1996**, *118*, 4488.
(13) Sullivan, P. A.; Axelsson, J.; Altmann, S.; Quist, A. P.; Sundqvist, B. U. R.; Reimann, C. T. *J. Am. Soc. Mass Spectrom.* **1996**, *7*, 329.
(14) Wyttenbach, T.; von Helden, G.; Bowers, M. T. *J. Am. Chem. Soc.* **1996**, *118*, 8355.
(15) Clemmer, D. E.; Hudgins, R. R.; Jarrold, M. F. *J. Am. Chem. Soc.* **1995**, *117*, 10141.
(16) Valentine, S. J.; Anderson, J. G.; Ellington, A. D.; Clemmer, D. E. *J. Phys. Chem. B* **1997**, *101*, 3891.
(17) Gross, D. S.; Schnier, P. D.; Rodriguez-Cruz, S. E.; Fagerquist, C. K.; Williams, E. R. *Proc. Natl. Acad. Sci. U.S.A.* **1996**, *93*, 3143.
(18) Klassen, J. S.; Blades, A. T.; Kebarle, P. *J. Phys. Chem.* **1995**, *99*, 15509.
(19) Kaltashov, I. A.; Fenselau, C. *Proteins: Struct., Funct., Genet.* **1997**, *27*, 165.
(20) Counterman, A. E.; Valentine, S. J.; Srebalus, C. A.; Henderson, S. C.; Hoaglund, C. S.; Clemmer, D. E. *J. Am. Soc. Mass Spectrom.* **1998**, *9*, 743.
(21) Dugourd, P.; Hudgins, R. R.; Clemmer, D. E.; Jarrold, M. F. *Rev. Sci. Instrum.* **1997**, *68*, 1122.
(22) Hudgins, R. R.; Woenckhaus, J.; Jarrold, M. F. *Int. J. Mass Spectrom. Ion Processes* **1997**, *165/166*, 497.
(23) Hagen, D. F. *Anal. Chem.* **1979**, *51*, 870.
(24) Karpas, Z.; Cohen, M. J.; Stimac, R. M.; Wernlund, R. F. *Int. J. Mass Spectrom. Ion Processes* **1986**, *74*, 153.
(25) Von Helden, G.; Hsu, M. T.; Kemper, P. R.; Bowers, M. T. *J. Chem. Phys.* **1991**, *95*, 3835.
(26) Clemmer, D. E.; Jarrold, M. F. *J. Mass Spectrom.* **1997**, *32*, 577.
(27) Mason, E. A.; McDaniel, E. W. *Transport Properties of Ions in Gases*; Wiley: New York, 1988.
(28) Brooks, B. R.; Bruccoleri, R. E.; Olafson, B. D.; States, D. J.; Swaminathan, S.; Karplus, M. *J. Comput. Chem.* **1983**, *4*, 187.
(29) Van Gunsteren, W. F.; Berendsen, H. J. *Mol. Phys.* **1977**, *34*, 1311.
(30) Gorman, G. S.; Speir, J. P.; Turner, C. A.; Amster, I. J. *J. Am. Chem. Soc.* **1992**, *114*, 3986.
(31) Wu, Z. C.; Fenselau, C. *Tetrahedron* **1993**, *49*, 9197.
(32) Mesleh, M. F.; Hunter, J. M.; Shvartsburg, A. A.; Schatz, G. C.; Jarrold, M. F. *J. Phys. Chem.* **1996**, *100*, 16082.

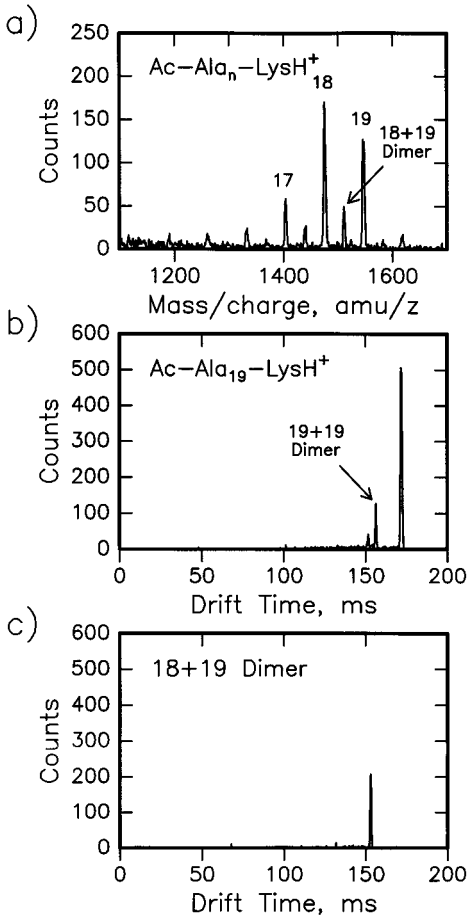

Figure 1. Electrospray mass spectrum of unpurified Ac-Ala$_{19}$-Lys (lysine at the C terminus) in formic acid (a) and drift time distributions measured at *m*/*z* corresponding to Ac-Ala$_{19}$-LysH$^+$ (b) and the (Ac-Ala$_{18}$-LysH·Ac-Ala$_{19}$-LysH)$^{2+}$ dimer (c).

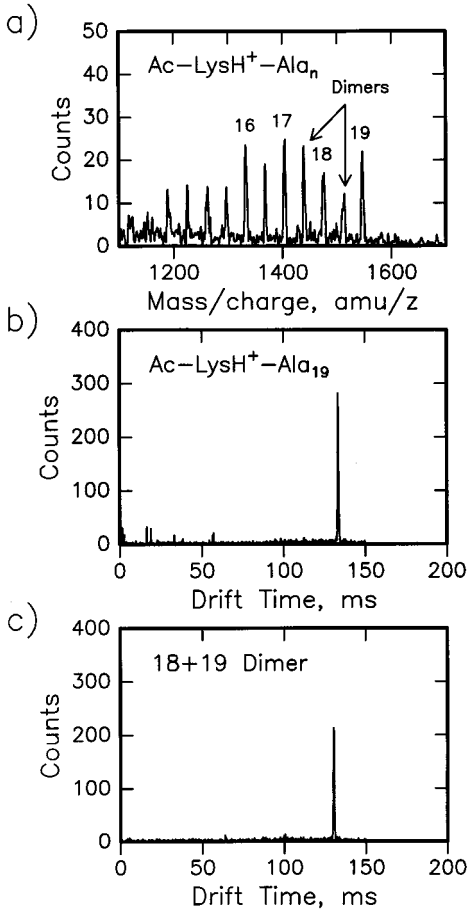

Figure 2. Electrospray mass spectrum of unpurified Ac-Lys-Ala$_{19}$ (lysine at the N terminus) in formic acid (a) and drift time distributions measured at *m*/*z* corresponding to Ac-LysH$^+$-Ala$_{19}$ (b) and the (Ac-LysH-Ala$_{18}$·Ac-LysH-Ala$_{19}$)$^{2+}$ dimer (c).

Experimental Results

Figure 1a shows a mass spectrum obtained by electrospraying a solution of unpurified Ac-Ala$_{19}$-Lys (lysine at the C terminus) in formic acid. There is a progression of peaks due to Ac-Ala$_n$-LysH$^+$, $n = 14-19$. Between these peaks there are smaller peaks that are assigned to dimers such as the 18 + 19 dimer, (Ac-Ala$_{18}$-LysH·Ac-Ala$_{19}$-LysH)$^{2+}$, which lies halfway between the $n = 18$ and 19 peaks. Parts b and c of Figure 1 show drift time distributions measured with the mass spectrometer set to transmit Ac-Ala$_{19}$-LysH$^+$ and the 18 + 19 dimer, respectively. In Figure 1c there is no analogue of the intense peak at ~170 ms in Figure 1b, while both distributions have peaks at ~150 ms. Since there is no monomer present at the same *m*/*z* (mass/charge) as the asymmetric 18 + 19 dimer, the peak at ~170 ms in Figure 1b must be due to the Ac-Ala$_{19}$-LysH$^+$ monomer. The smaller peaks at ~150 ms in Figure 1b must be due to dimers which occur at the same *m*/*z* as the $n = 19$ monomer. The larger dimer peak in Figure 1b is almost certainly due to (Ac-Ala$_{19}$-LysH)$_2^{2+}$, whereas the smaller one is probably due to an 18 + 20 dimer.

Figure 2a shows a mass spectrum measured by electrospraying unpurified Ac-Lys-Ala$_{19}$ (lysine at the N terminus) in formic acid. There are peaks with *m*/*z* ratios corresponding to Ac-LysH$^+$-Ala$_n$ monomers and to asymmetric dimers, (Ac-LysH-A$_n$·Ac-LysH-A$_{n+1}$)$^{2+}$. Unlike the spectrum shown in Figure 1a, these two sets of peaks have similar intensities. Drift time distributions measured at *m*/*z* corresponding to the Ac-LysH$^+$-Ala$_{19}$ monomer and the asymmetric 18 + 19 dimer are shown in Figure 2b and 2c, respectively. There is only a single peak present in both distributions, and they have similar drift times. Since the peak in Figure 2c is due to the (Ac-LysH-Ala$_{18}$·Ac-LysH-Ala$_{19}$)$^{2+}$ dimer, the peak in Figure 2b must be due to an (Ac-LysH-Ala$_{19}$)$_2^{2+}$ dimer. Thus, there is no monomer present for the Ac-LysH$^+$-Ala$_{19}$ peptide. Measurements were performed with the electrosprayed solution diluted by a factor of up to 10, but no new peaks were observed. The complete absence of a monomer peak suggests that the dimer is present in solution, because whereas some dimerization may occur in the process of electrospraying the peptides, complete dimerization seems unlikely if not impossible. Complete dimerization was not observed for the Ac-Ala$_n$-LysH$^+$ peptides where the same peptide concentrations were used. Cross sections determined for the (Ac-LysH-Ala$_n$)$_2^{2+}$ dimers are plotted in Figure 3. Cross sections for the (Ac-Ala$_n$-LysH)$_2^{2+}$ dimers mentioned above are plotted in the same figure. The (Ac-Ala$_n$-LysH)$_2^{2+}$ dimers (with the lysine at the C terminus) have significantly larger cross sections than the (Ac-LysH-Ala$_n$)$_2^{2+}$ dimers (with the lysine at the N terminus).

Drift time distributions recorded at *m*/*z* corresponding to Ac-LysH$^+$-Ala$_n$ with $n = 11-15$ are shown in Figure 4. Note that the peaks systematically shift to slightly smaller times with decreasing peptide size because of the decrease in the size of the ions. The distribution measured at *m*/*z* corresponding to Ac-LysH$^+$-Ala$_{15}$ has a single peak that is the analogue of the dimer peak present for Ac-LysH$^+$-Ala$_{19}$ in Figure 2b. However, in the distribution recorded at *m*/*z* corresponding to Ac-LysH$^+$-Ala$_{13}$ a second peak has appeared at a longer time. For $n < 13$ the analogue of the peak assigned to the (Ac-LysH-Ala$_n$)$_2^{2+}$

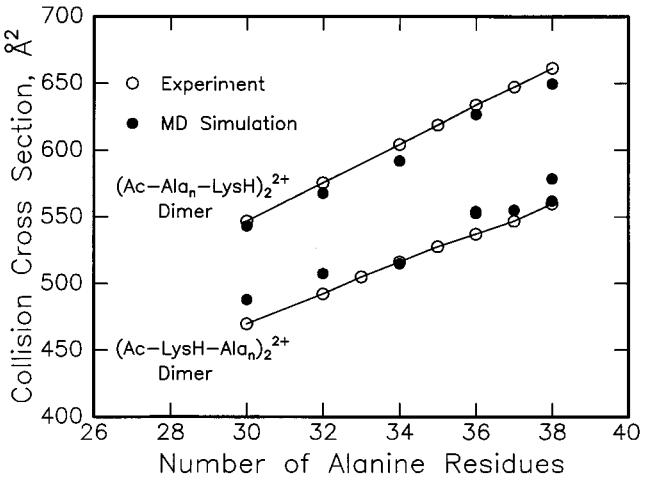

Figure 3. Plot of the cross sections for the (Ac-Ala$_n$-LysH)$_2^{2+}$ and (Ac-LysH-Ala$_n$)$_2^{2+}$ dimers against the number of alanine residues. Cross sections calculated for the antiparallel head-to-toe helical dimer of Ac-LysH$^+$-Ala$_n$ and the (Ac-Ala$_n$-LysH)$_2^{2+}$ dimer with two helices connected in a nearly collinear (or vee-shaped) arrangement (see text) are shown for comparison with the measured cross sections.

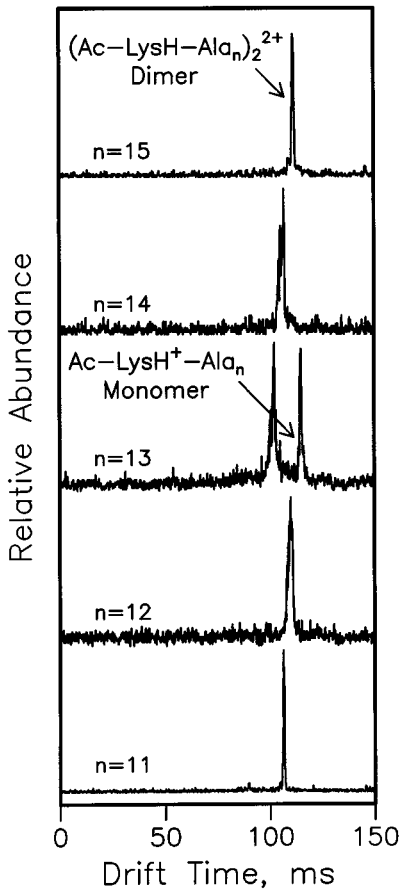

Figure 4. Drift time distributions measured at *m/z* corresponding to Ac-LysH$^+$-Ala$_n$ peptides with $n = 11-15$.

dimer is no longer present, and the distribution is dominated by the peak at longer time. This peak appears to be due to the Ac-LysH$^+$-Ala$_n$ monomer. At around $n = 13$ the asymmetric dimer peaks, (Ac-LysH-Ala$_n$·Ac-LysH-Ala$_{n+1}$)$^{2+}$, vanish from the mass spectrum, and the separation between the main peaks becomes consistent with the presence of monomers. The dimer occurs at shorter drift times than that of the monomer because it is doubly charged. The monomer to dimer transition observed

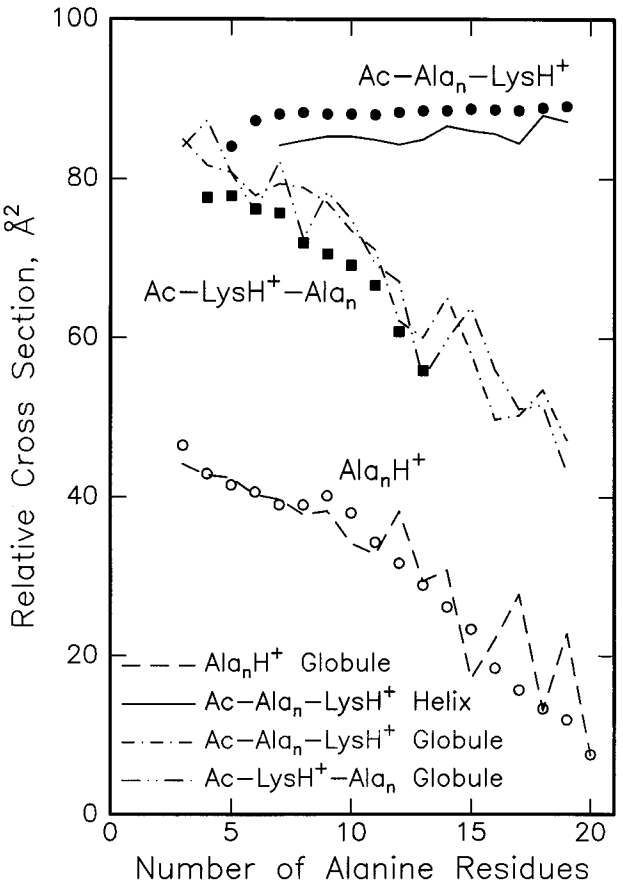

Figure 5. Plot of the relative cross sections for Ala$_n$H$^+$ (○), Ac-Ala$_n$-LysH$^+$ (●), and Ac-LysH$^+$-Ala$_n$ (■) peptides against the number of alanine residues. The relative cross section scale is given by $\Omega_{av}^{(1,1)} - 14.50n$ where the cross section, $\Omega_{av}^{(1,1)}$, is in Å^2 and 14.50 Å^2 is the calculated average cross section per residue for an ideal polyalanine α-helix. Cross sections calculated for Ac-Ala$_n$-LysH$^+$ helices and Ala$_n$H$^+$, Ac-Ala$_n$-LysH$^+$, and Ac-LysH$^+$-Ala$_n$ globules are shown for comparison with the measured cross sections.

here is remarkably sharp, the monomer and dimer only coexist for $n = 13$.

Relative collision cross sections for Ala$_n$H$^+$, $n = 3-20$ (from ref 9), Ac-Ala$_n$-LysH$^+$, $n = 5-19$, and monomeric Ac-LysH$^+$-Ala$_n$, $n = 4-13$, are plotted against n in Figure 5. The relative cross section scale employed here is given by $\Omega_{av}^{(1,1)} - 14.50n$ where the cross section, $\Omega_{av}^{(1,1)}$, is in Å^2 and 14.50 Å^2 is the average cross section per residue determined for an ideal polyalanine α-helix with the torsion angles fixed at $\phi = -57°$ and $\psi = -47°$. With this relative cross section scale, helical conformations have relative cross sections that are independent of the number of alanine residues whereas other conformations have relative cross sections that change with the number of residues. The relative cross sections measured for the Ac-Ala$_n$-LysH$^+$ peptides (with the lysine at the C terminus) are independent of n for $n \geq 7$, indicating that these peptides have helical conformations. On the other hand, the relative cross sections for the Ala$_n$H$^+$ and Ac-LysH$^+$-Ala$_n$ peptides clearly decrease with increasing size, indicating that these peptides have conformations that are more compact than helices.

Ac-Ala$_n$-LysH$^+$ Monomers. MD simulations indicate that the helical conformation is stable for the larger Ac-Ala$_n$-LysH$^+$ peptides (with the lysine at the C terminus). A representative structure from the simulations for Ac−Ala$_{19}$-LysH$^+$ is shown in Figure 6a. In an ideal helix, the last four carbonyl groups at

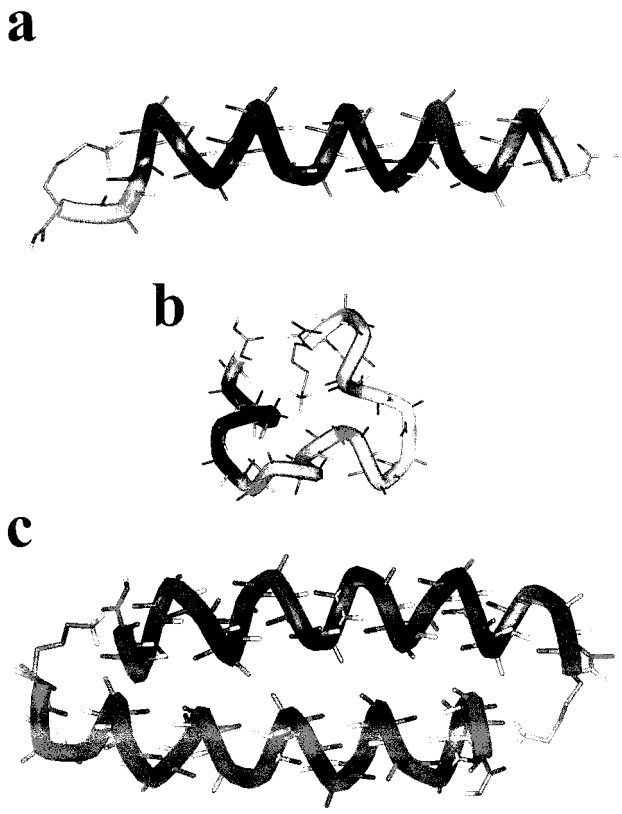

Figure 6. Representative structures from the MD simulations: (a) Ac-Ala_{19}-$LysH^+$ helix; (b) Ac-$LysH^+$-Ala_{19} globule; and (c) (Ac-LysH-Ala_{19})$_2^{2+}$ antiparallel head-to-toe helical dimer.

the C terminus do not have hydrogen-bonding partners. The Ac-Ala_n-$LysH^+$ helices are stabilized by hydrogen bonds between the protonated amine group of the lysine and the dangling carbonyl groups at the C terminus. Hydrogen-bonding partners are believed to stabilize helices within proteins[33,34] and there is evidence for similar helix-capping effects for small peptides in solution.[35] The helical conformation in Figure 6a is further stabilized by a favorable interaction between the charge and the helix dipole. An α-helix has a substantial macrodipole (equivalent to around half an elementary charge at each end) that results from the near perfect alignment of the dipoles of the individual peptide units along the length of the helix.[36] Both theory and solution studies indicate that it is more favorable to locate amino acids with charged side chains near the end of the helix dipole with opposite polarity.[33,35,37,38]

Cross sections calculated for the helical conformations of the Ac-Ala_n-$LysH^+$ peptides are plotted as the solid line in Figure 5. They are in good agreement with the measured cross sections. Globular conformations were generated for the Ac-Ala_n-$LysH^+$ peptides by starting the simulations from extended strings ($\phi = \psi = 180°$). The globular conformations are significantly higher in energy than the helices and at the start of some of the simulations the extended conformations collapsed directly into helices. Calculated cross sections for the Ac-Ala_n-$LysH^+$ globules are shown in Figure 5. The relative cross sections decrease with increasing peptide size, since the globules are more compact than helices

Ac-$LysH^+$-Ala_n Monomers. The helical conformation is not stable in MD simulations for the Ac-$LysH^+$-Ala_n peptides (with the lysine at the N terminus). Simulations started from an ideal helix rapidly collapse to globular conformations, usually within the first 100 ps. An example of a globular conformation for Ac-$LysH^+$-Ala_{19} is shown in Figure 6b. Many different globular conformations were found with the peptide wrapped up around the charge site. This structural motif has been observed in previous simulations for much smaller peptides,[18,39] and in simulations of larger protonated polyalanine and polyglycine peptides.[9] Some of the globules, like the one shown in Figure 6b, have short helical regions. Short helical regions were also found in simulations for the larger Ala_nH^+ peptides.[9] The peptides with the lysine at the N terminus (Ac-$LysH^+$-Ala_n) adopt globular conformations because the helix-capping interactions and charge−dipole interactions that stabilize the Ac-Ala_n-$LysH^+$ helices are absent. In fact, the location of the charge at the N terminus of the Ac-$LysH^+$-Ala_n peptides destabilizes the helical conformation. This is also true for the protonated polyalanine peptides (because it is the N terminus that is protonated) and explains why the helical conformation is not stable for the Ala_nH^+ peptides. Relative cross sections calculated for the Ac-$LysH^+$-Ala_n globules are plotted in Figure 5. They are similar to the cross sections calculated for the Ac-Ala_n-$LysH^+$ globules. The relative cross sections decrease with increasing peptide size because the globules are more compact than helices. The calculated cross sections for the globules are in reasonable agreement with cross sections measured for the monomeric Ac-$LysH^+$-Ala_n, $n = 4-13$, peptides. Note that there are large fluctuations in the cross sections calculated for the globules. This results from the limited time scale of the MD simulations. There are an enormous number of globular conformations, and it is unlikely that we have found the lowest energy ones in our simulations. However, identification of the lowest energy conformation is probably not relevant because MD simulations indicate that at room temperature the peptides are interconverting rapidly between many different globular conformations.[9] In other words, they do not have a well-defined structure. Cross sections calculated for the Ala_nH^+ globules are also plotted in Figure 5, and they are in good agreement with the measured cross sections for these peptides.

Relative Energies of the Helices and Globules. Figure 7 shows a plot of the relative energies of the Ac-Ala_n-$LysH^+$ helices and Ac-$LysH^+$-Ala_n globules. The relative energy scale used here was obtained by subtracting the energy of Ac-Ala_n-$LysH^+$ globules from the energies of the other conformations. We used the lowest energy found in two or more simulations performed for each conformation. The energies of the Ac-Ala_n-$LysH^+$ and Ac-$LysH^+$-Ala_n globules are similar and thus the relative energies of the Ac-$LysH^+$-Ala_n globules fluctuate around 0 kJ mol^{-1} in Figure 7. The fluctuations result from the limited time scale of the MD simulations. The relative energies for the Ac-Ala_n-$LysH^+$ helices decrease with increasing peptide size. According to the simulations, the helix is around 150 kJ mol^{-1} more stable than the globule for Ac−Ala_{19}-$LysH^+$. This energy difference decreases to be less than 50 kJ mol^{-1} for $n < 8$. However, these energies are not free energies, and there is a considerable entropy cost associated with helix formation. According to recent estimates from Monte Carlo simulations using a multicanonical ensemble,[40] the $T\Delta S$ terms for the helix-

(33) Presta, L. G.; Rose, G. D. *Science* **1988**, *240*, 1632.
(34) Seale, J. W.; Srinivasan, R.; Rose, G. D. *Protein Sci.* **1994**, *3*, 1741.
(35) Forood, B.; Feliciano, E. J.; Nambiar, K. P. *Proc. Natl. Acad. Sci. U.S.A.* **1993**, *90*, 838.
(36) Hol, W. G. J.; vanDuijnen, P. T.; Berendsen, H. J. C. *Nature (London)* **1978**, *273*, 443.
(37) Blagdon, D. E.; Goodman, M. *Biopolymers* **1975**, *14*, 241.
(38) Daggett, V. D.; Kollman, P. A.; Kuntz, I. D. *Chem. Scr.* **1989**, *29A*, 205.
(39) Wyttenbach, T.; Bushnell, J. E.; Bowers, M. T. *J. Am. Chem. Soc.* **1998**, *120*, 5098.
(40) Okamoto, Y.; Hansmann, U. H. E. *J. Phys. Chem.* **1995**, *99*, 11276.

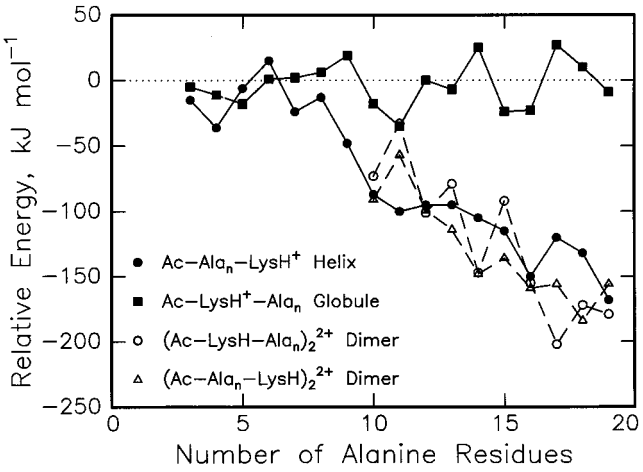

Figure 7. Plot of the relative energies determined from the MD simulations for the Ac-Ala$_n$-LysH$^+$ helices, Ac-LysH$^+$-Ala$_n$ globules, the (Ac-LysH-Ala$_n$)$_2^{2+}$ antiparallel head-to-toe helical dimers, and the (Ac-LysH-Ala$_n$)$_2^{2+}$ dimers with two helices connected in a nearly collinear (or vee-shaped) arrangement. The relative energies were obtained by subtracting the energies of the Ac-Ala$_n$-LysH$^+$ globules. For the dimers the relative energies are per monomer unit.

to-coil (or globule) transition in a vacuum at 300 K are −18.8, −59.4, and −115.5 kJ mol^{-1} for Ala$_{10}$, Ala$_{15}$, and Ala$_{20}$, respectively. These values should provide a reasonable estimate of the $T\Delta S$ terms for the lysine-containing analogues. By taking into account the $T\Delta S$ term, the simulations are still found to favor the helix as the lowest free-energy structure at room temperature for Ac-Ala$_n$-LysH$^+$ peptides with n ≥ 9, in agreement with the experimental results. From the measured relative cross sections shown in Figure 5, the first peptide to deviate significantly from the line provided by the larger peptides is Ac−Ala$_6$-LysH$^+$, which suggests that Ac-Ala$_n$-LysH$^+$ peptides with n as small as 7 are predominantly helical. A helical peptide with eight residues ($n = 7$) is much smaller than any helical peptide found in solution. Even small helical peptides such as the 13-residue C-peptide (analogue III) of RNAse A only exhibit ≤25% helicity in solution at room temperature.[41] This supports the idea that secondary structure is more stable in vacuo than in solution.

(Ac-LysH-Ala$_n$)$_2^{2+}$ Dimers. Only dimers are observed for the larger Ac-LysH$^+$-Ala$_n$ peptides (with the lysine at the N terminus). Since the helix is so much more stable than the globule for the larger Ac-Ala$_n$-LysH$^+$ peptides (with the lysine at the C terminus) the most likely conformation for the Ac-LysH$^+$-Ala$_n$ dimers that dominate for $n > 13$ is two helices in a head-to-toe arrangement with the lysine from one peptide interacting with the C terminus of the other. This geometry incorporates all of the helix-stabilizing features of the Ac-Ala$_n$-LysH$^+$ peptides (with the lysine at the C terminus), and furthermore, the helices are antiparallel so that the interaction between their dipoles is favorable. Figure 6c shows a typical conformation from MD simulations of the (Ac-LysH-Ala$_{19}$)$_2^{2+}$ dimer that were started from a geometry of two antiparallel helices. The relative energies determined from the MD simulations for this dimer are shown in Figure 7. Note that the relative energies are per monomer unit. Not surprisingly, the relative energies are similar to those for the Ac-Ala$_n$-LysH$^+$ helices. For Ac-LysH$^+$-Ala$_{19}$, the head-to-toe helical dimer conformation is around 175 kJ mol^{-1} per monomer unit more stable than the monomeric globule. In other words the reaction:

$$\underset{\text{(globule)}}{\text{Ac-LysH}^+\text{-Ala}_{19}} + \underset{\text{(globule)}}{\text{Ac-LysH}^+\text{-Ala}_{19}} \rightarrow \underset{\text{(helical dimer)}}{(\text{Ac-LysH-Ala}_{19})_2^{2+}} \quad (2)$$

is exothermic by around 350 kJ mol^{-1}. However, it is the free-energy change that is important here, and we need to account for the entropy change associated with helix formation. There is also an additional entropy term for the association reaction which results from the loss of translational entropy as two monomers combine to give a dimer. This contributes a $T\Delta S$ term of −60 kJ mol^{-1} at room temperature (in a vacuum). Using the value of −115 kJ mol^{-1} estimated for the $T\Delta S$ term for the helix-to-coil transition in Ala$_{20}$ at room temperature,[40] the free-energy change associated with forming an (Ac-LysH-Ala$_{19}$)$_2^{2+}$ helical dimer is estimated to be around −60 kJ mol^{-1}. This is consistent with the helical dimer being dominant for the larger Ac-LysH$^+$-Ala$_n$ peptides. The calculated cross sections for the antiparallel helical dimers are compared with the measured cross sections in Figure 3. In some cases the calculated cross sections are in good agreement with the measured values, whereas in others the calculated values are too large by around 3%. The difference seems to be the separation between the helices. The dimers that are the best fit to the experimental values have interhelical spacings of ∼8 Å. For the dimers with the larger cross sections, the interhelical spacings are ∼1 Å larger. An interhelical spacing of 8.1 Å was previously found by molecular mechanics calculations to be the minimum energy spacing for two antiparallel polyalanine helices.[42] The larger spacing found in some of the simulations probably results from steric problems in locating the lysine of one monomer favorably at the C terminus of the other. The close interhelical spacing inferred from the experiments suggests that the dimers are stabilized by significant interhelical interactions, in addition to the terminal interactions.

In addition to the helical dimer described above we considered a variety of other conformations as candidates for the geometries of the (Ac-LysH-Ala$_n$)$_2^{2+}$ dimers. Results for some of these conformations are shown in Table 1. The head-to-toe helical dimer is by far the lowest energy conformation found. Globular conformations are all substantially higher in energy. A globular conformation started from two Ac-LysH$^+$-Ala$_{19}$ globules is shown in Figure 8a. The energy of this conformation is not substantially lower than that of two isolated globules.

For monomeric Ac-Ala$_n$-LysH$^+$ the smallest helical peptide appears to be for $n = 7$. While for the Ac-LysH$^+$-Ala$_n$ peptides there is a sharp transition between helical dimers and globular monomers at $n = 13$. The principle difference between the helix to globule transition in the monomeric Ac-Ala$_n$-LysH$^+$ peptides and the transition between helical dimers and monomeric globules in the Ac-LysH$^+$-Ala$_n$ peptides is the additional entropy term for the helical dimers which results from the loss of translational entropy as two monomers combine. This additional entropy term is why the transition from helical dimers to globular monomers occurs for larger peptides than the helix to globule transition in the monomeric Ac-Ala$_n$-LysH$^+$ peptides.

(Ac-Ala$_n$-LysH)$_2^{2+}$ Dimers. Dimers are present in the experiments for the larger Ac-Ala$_n$-LysH$^+$ peptides but they are not as abundant as for the Ac-LysH$^+$-Ala$_n$ peptides. A variety of different conformations were examined for the (Ac-Ala$_n$-LysH)$_2^{2+}$ dimers, and the results for some of them are summarized in Table 1. Two low-energy conformations were found. One is a dimer consisting of two helices with the lysine

(41) Shoemaker, K. R.; Kim, P. S.; York, E. J.; Stewart, J. M.; Baldwin, R. L. *Nature* **1987**, *326*, 563.

(42) Silverman, D. N.; Scheraga, H. A. *Arch. Biochem. Biophys.* **1972**, *153*, 449.

Table 1. Comparison of the Cross Sections and Energies of a Variety of Conformations for the $(Ac\text{-}LysH\text{-}Ala_{19})_2^{2+}$ and $(Ac\text{-}Ala_{19}\text{-}LysH)_2^{2+}$ Dimers

	cross section, Å^2	energy, kJ mol^{-1}
$(Ac\text{-}LysH\text{-}Ala_{19})_2^{2+}$ dimers		
experiment	560	
antiparallel head-to-toe helices (see Figure 7c)	562	−5674
globule started from two globules (see Figure 8a)	538	−5341
globule started from antiparallel extended strings	593	−5239
$(Ac-Ala_{19}\text{-}LysH)_2^{2+}$ dimers		
experiment	661	
helices connected nearly collinear (or vee-shaped) (see Figure 8b)	653	−5666
two antiparallel helices (see Figure 8c)	566	−5658
globule started from two globules	513	−5289
globule started from antiparallel extended strings	549	−5346

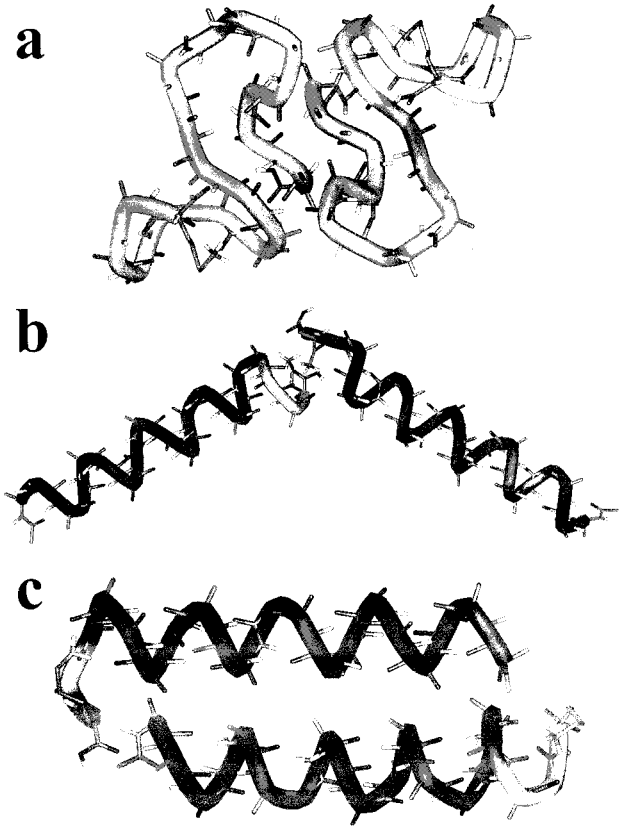

Figure 8. Representative structures from the MD simulations: (a) $(Ac\text{-}LysH\text{-}Ala_{19})_2^{2+}$ dimer started from two globules; (b) $(Ac\text{-}Ala_{19}\text{-}LysH)_2^{2+}$ dimer with two helices connected in a nearly collinear (or vee-shaped) arrangement; and (c) $(Ac\text{-}Ala_{19}\text{-}LysH)_2^{2+}$ dimer with two antiparallel helices.

of one peptide interacting with the C terminus of the other. This conformation is shown in Figure 8b. The helices are arranged in a nearly collinear (or vee-shaped) arrangement to minimize unfavorable electrostatic interactions between the helix dipoles. A side-by-side arrangement of the helices is unfavorable here because the helix dipoles would be parallel. The vee-shaped dimer resulted from simulations started with the helices in a side-by-side conformation with parallel helix dipoles, as well as a collinear initial conformation with the two C-termini facing each other. The other low-energy conformation found for the $(Ac\text{-}Ala_n\text{-}LysH)_2^{2+}$ dimers has two helices arranged antiparallel.

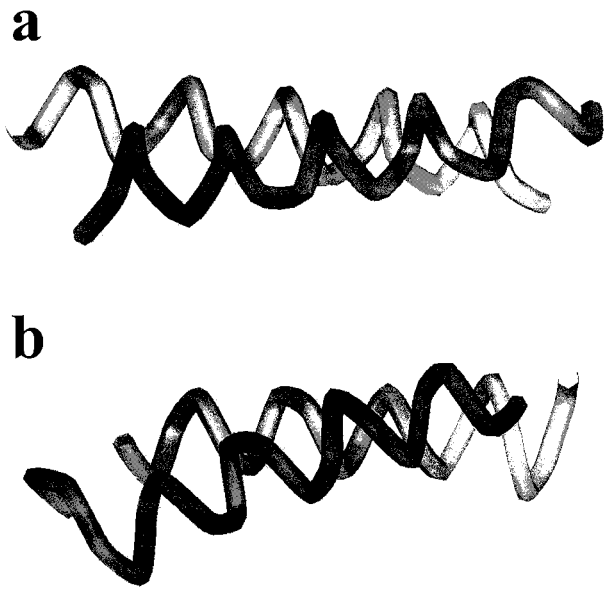

Figure 9. Side view of some helical dimers from the MD simulations: (a) $(Ac\text{-}LysH\text{-}Ala_{19})_2^{2+}$ antiparallel head-to-toe helical dimer (from Figure 6c); and (b) $(Ac\text{-}Ala_{19}\text{-}LysH)_2^{2+}$ dimer with two antiparallel helices (from Figure 8c). The atoms have been removed for clarity.

This conformation is shown in Figure 8c. Here, the lysines interact with the C terminus on the same peptide, and the dimer is bound by electrostatic interactions between the helix dipoles, as well as by weak side chain interactions, and occasionally, by additional hydrogen bonds at the termini. From the energies shown in Table 1, the antiparallel helix has almost the same energy as the nearly collinear (or vee-shaped) arrangement. Thus, it is not clear from the simulations which of these two helical dimer conformations has the lower energy. However, calculated cross sections for the antiparallel helices, Figure 8c, are not close to the measured cross sections, whereas cross sections calculated for the near collinear (or vee-shaped) arrangement, Figure 8b, are in good agreement with experiment (see Table 1). This indicates that the dimer present in the experiments is probably the one with the nearly collinear (or vee-shaped) arrangement. Cross sections calculated for this conformation are compared with the experimental data in Figure 3. The calculated cross sections are slightly smaller than the measured ones, the root-mean-square deviation is 1.5%. This dimer is quite floppy, and the small discrepancy could easily result from the simulations not getting the angle between the helices quite right.

Formation of the near collinear (or vee-shaped) helical dimers from helical monomers requires uncoupling of the lysine caps from both peptides and then interchanging the lysine side chains. It is difficult to imagine this process happening quickly or without a sizable activation barrier. The presence of an activation barrier would explain why these dimers are observed since they are not predicted to be very stable toward dissociation into helical monomers. On the other hand, the other low-energy dimer geometry found for the $Ac\text{-}Ala_n\text{-}LysH^+$ peptides, the one with antiparallel helices, should not have a significant activation barrier for dissociation into helical monomers because the helices are not coupled by strong hydrogen bonds. It is plausible that this geometry also exists in solution, but it dissociates in the gas phase in a time substantially less than the time scale of the experiments.

Helix−Helix Interactions. In the simulations of the dimers with antiparallel helices there is a significant angle between the axes of the helices. Figure 9a and b shows side views of the

$(Ac\text{-}LysH\text{-}Ala_{19})_2^{2+}$ antiparallel head-to-toe helical dimer (from Figure 6c) and the $(Ac\text{-}Ala_{19}\text{-}LysH)_2^{2+}$ antiparallel helical dimer (from Figure 8c), respectively. The atoms have been removed for clarity. An interhelical angle of around 20° seems to result from a favorable packing arrangement between the alanine side chains of the two monomers. This interhelical angle results in a "coiled-coil" geometry where the two helices are twisted together.[43] Typically, coiled coils are observed either in very long, fibrous proteins, or as part of the tertiary structure of a protein.[44] The dimers studied here are short coiled coils without stabilization from additional tertiary forces or peripheral molecules. Thus, the gas phase may be an ideal environment for studying supersecondary structure, as well as secondary structure.

Acknowledgment. We thank Jiri Kolafa for the use of his PROSIS simulation software. We gratefully acknowledge the support of the Petroleum Research Fund, administered by the American Chemical Society, and support by the National Science Foundation.

JA983996A

(43) Crick, F. H. C. *Acta Crystallogr.* **1953**, *6*, 689.

(44) Lupas, A. *TIBS* **1996**, *21*, 375.